Transaction B: Mechanical Engineering
Vol. 16, No. 5, pp. 451–462

SCIENTIA IRANICA

Estimation of Human Lower Extremity Musculoskeletal Conditions During Backpack Load Carrying

A. Selk Ghafari[1], A. Meghdari[1,*] and G.R. Vossughi[1]

Abstract. *This paper focuses on the biomechanical aspects of the human lower extremity loading condition during backpack load carrying. A biomechanical framework was generated with the aim of employing a block-oriented structure of Simulink integrated with the Virtual Reality Toolbox of MATLAB software to provide a simulation study of the musculoskeletal system in a virtual environment. In this case, a ten-degrees-of-freedom musculoskeletal model actuated with sixteen muscles in each leg was utilized to simulate movement in the sagittal plane. An inverse dynamics based optimization approach was employed to estimate the excitation level of the muscles. In addition, distributions of the mechanical power analysis for lower extremity muscles were carried out to enhance the understanding of human leg morphology and control mechanism to provide load support. Simulation results provide a biomechanical framework to identify the muscles and joints, which are critically subjected to musculoskeletal injuries during the activity under investigation. Analysis of the muscle activation patterns and their distribution of the mechanical powers revealed the important role of the plantar flexors of the ankle and the extensors of the knee and hip joints in supporting the body during backpack load carrying.*

Keywords: *Lower extremity; Musculoskeletal; Backpack; Load carrying; Muscle activation.*

INTRODUCTION

The action of muscles during normal activities produces bone loading and joint contact forces in surplus of body weight [1]. Musculoskeletal loading is influenced by a number of inter-individual factors, such as weight and gender [2] as well as the activity being undertaken [3,4]. Determining in vivo loading conditions in human joints is difficult due to the combination of complex structural anatomy, complicated movement and dynamics and often indeterminate muscle function. As a result, mathematical models have been employed to estimate various activities, such as muscle and joint contact forces [5-7], contribution of the lower extremity muscles to body support and forward progression and swing leg kinematics during walking [8-10]. A model based estimation of muscle force usually requires optimization regardless of the inverse or forward dynamic strategies selected to solve the governing equations of the musculoskeletal system [11,12]. The redundancy of muscular load sharing can be addressed by minimizing an objective function appropriately selected for the movement under investigation. Both static and dynamic optimization approaches have been employed with equivalent results for normal gait [13]. One of the most interesting problems in biomechanical studies is investigation of the main functional differences of lower extremity muscles for various activities [14]. These studies contain informative biomechanical aspects and reveal the contribution of individual muscles for load sharing, body support and the provision of body forward progression during the movements under investigation. Musculoskeletal systems were extensively utilized to study the relationship between impaired muscle coordination and observed gait deviations in people with paretic muscles [15]. Carrying heavy loads is one of the most common reasons behind the leading cause of musculoskeletal injuries. Peoples employed

1. *Center of Excellence in Design, Robotics and Automation, School of Mechanical Engineering, Sharif University of Technology, Tehran, P.O. Box 11155-9567, Iran.*
*. *Corresponding author. E-mail: meghdari@sharif.edu*

Received 7 July 2008; received in revised form 8 March 2009; accepted 18 April 2009

in specific occupations, such as fire-fighters in hauling heavy equipment upstairs, nurses and physiotherapists lifting patients on and off beds or people who assist medical personnel in carrying wounded people from disaster areas, often have to carry heavy loads. Furthermore, foot soldiers often have to carry extremely heavy backpack loads and walk long distance in rough terrain. Much research has been carried out into the effects of the configuration of load carriage on the kinematics and kinetics of lower extremities [16], joint forces [17], the energy expenditure of locomotion [18,19], ground reactions [20] and the electromyographic activities of back muscle groups [21]. To the authors' knowledge, there is no extensive study in the literature regarding the musculoskeletal analysis of the lower extremity during load carrying. Dynamic simulation of human movement under load carrying conditions not only offers a powerful methodology for characterization of the causal relationship between muscle excitation patterns and the movement under investigation, but also provides a framework to perform appropriate rehabilitation processes needed to improve gait abnormalities. This paper describes the contributions of the lower extremity muscles under load carrying conditions with the aim of developing a musculoskeletal model of the body. Activation levels of the lower extremity muscles were simulated employing an inverse dynamics based optimization approach. In addition, distribution of a mechanical power analysis for individual muscles was carried out to investigate the main functional differences between level walking and load carrying. Biomechanical analysis of the movement under investigation enhances the understanding of human leg morphology and control mechanism in supporting loads and provides a biomechanical framework to identify the muscles and joints that are critically subjected to musculoskeletal injury during load carrying. In addition, muscle energy highlights the design criterion of more efficient, anthropometric and lightweight assistive device structures for load augmentation purposes. The appropriate actuation mechanism of such a system should provide an additional plantar flexion torque in the ankle joint and an extension torque in knee and hip joints. Besides, the results provide a useful tool to perform appropriate rehabilitation processes needed to improve gait performance after injuries sustained in the musculoskeletal system during load carrying.

MUSCULOSKELETAL MODEL

A complete musculoskeletal model of the human lower extremity was developed with the aim of employing MATLAB/Simulink and the Virtual Reality Toolbox. A three-dimensional model of lower extremity bones was constructed, based on collected data from medical imaging, mainly by a Computer Tomography (CT) scan. Surfaces of the lower limb bones involving the left and right iliac bones, the femur, the patella, the tibia, the fibula and all bones of the foot were reconstructed. Then, a model of the Head, Arms and Torso (HAT) was generated as a single rigid body. The constraints of the motion were applied to the model, based on the anatomical center of rotation of the joints. A total of 23 degrees-of-freedom was considered to describe the motion of the musculoskeleton in three-dimensional space. HAT was articulated with the pelvis via a three degrees-of-freedom joint located at the third lumbar vertebra. Each hip joint was modeled as a three degrees-of-freedom ball and socket joint. For the knee joint, a modified planar model characterizing the knee extensor mechanism [22] was employed. The foot was modeled as a single segment which was articulated with the tibia via a three degrees-of-freedom rotational joint. Also, six degrees-of-freedom were assigned to the HAT position and orientation relative to the ground. Twenty functional muscle groups, based on anatomical classification, were employed to drive the model. The muscle groups included in the model were GMAX (gluteus maximus, adductor magnus), IL (iliacus, psoas), HA (biceps femoris long head, medial hamistrings), VS (three-component vasti), RF (rectus femoris), BF (biceps femoris short head), TA (tibialis anterior), TP (tibialis posterior), GA (medial and lateral gastrocnemius) and SO (soleus). An orthogonal reference frame for each segment is assigned in the anatomical joint location, based on the data provided in the literature [23]. The reference frames assigned in the proposed model are characterized by the pelvis (PEL) which is fixed at the midpoint of the line connecting the two anterior superior iliac spines, Femur (FEM) which is fixed at the center of the femoral head, Tibia (TIB) which is located at the mid point of the line between the medial and lateral femoral epicondyles, Talus (TAL) and Foot (F) which are located at the mid point of the line between the apices of the medial and lateral malleolus. The origin and direction of the segmental reference frames in the skeletal model are illustrated in Figure 1a. The origin and insertion coordinates for each actuator were defined based on the assigned segmental reference frames to describe the attachment sites of muscles on the proposed skeletal model. Coordinates data for the muscles included in the proposed model are given in the Appendix (Tables A1 and A2) [23]. In some cases, it is sufficient to describe the muscle path with a line segment between the origin and the insertion points. In other cases, where the muscle wraps over bone or is constrained by retinacula, intermediate points, or effective origin and insertion points, were introduced to represent the muscle path more accurately [23,24]. The proposed musculoskeletal model and muscle groups included in the model are illustrated in Figure 1b. The

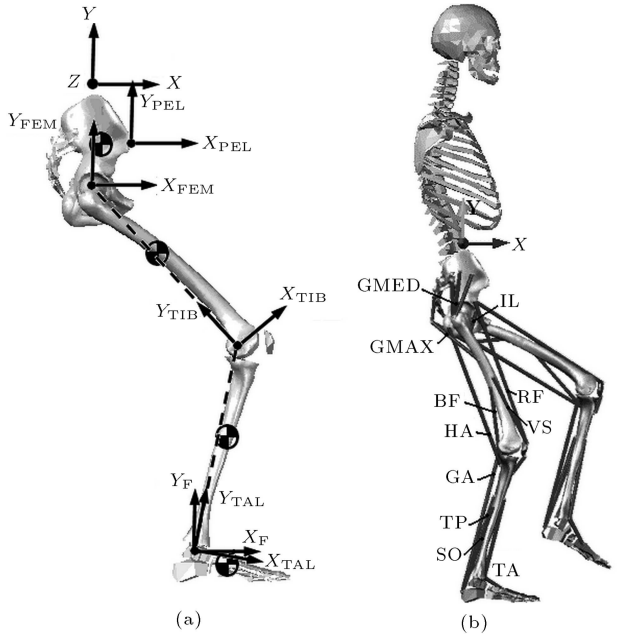

Figure 1. (a) Segmental reference frames of the right lower extremity. Origins and directions of the orthogonal reference frames are shown for the pelvis (PEL), femur (FEM), tibia (TIB), talus (TAL) and foot (F); (b) the musculoskeletal model of the lower extremity and muscle groups included in the model.

muscles within each group received the same excitation pattern. The force generating capacity of each actuator was considered based on a Hill-type model governed by muscle force-length-velocity characteristics [24]. In the proposed model, in addition to the active element, there is a passive viscoelastic element in parallel and an elastic tendon element in series. The muscle excitation-contraction dynamics were modeled using a first order differential equation to relate the rate of change in activation to the muscle excitation signal, based on a description from the literature [24]. In the proposed model, the activation level of the muscles can be varied continuously between zero and one; zero indicating no excitation and one indicating full excitation. For a graphic representation of the musculoskeletal system, the constructed model was exported in a WRL format which served as the input file of the Virtual Reality toolbox of MATLAB [25].

Since the flexion-extension degrees of freedom at ankle, knee and hip joints are subjected to the highest amount of power [26,27], the simulation analysis was constrained to the sagittal plane movement. Accordingly, a total of ten degrees-of-freedom was considered to represent the motion of the musculoskeletal system. The governing equations of the musculoskeletal system were generated employing a vector bond-graph approach [28]. The application of vector bond graphs to multi-body dynamic systems significantly reduces the amount of effort required to model such systems. Each segment of the lower extremity is subjected to muscle forces, thus the effects of the muscle forces can be replaced by an external force and moment about each anatomical joint center. The segment's mass and inertia are indicated by m_i and J_i, respectively, and the body coordinate system is located at the center of mass of the rigid body. The arm vectors from joint $i-1$ and i to the center of mass of segment i are defined by R_{i-} and R_{i+}, respectively. A corresponding vector bond graph model for the rigid body segment illustrated in Figure 2a is proposed as the system depicted in Figures 2b and 2c [29]. In the proposed bond graph model, the revolute joints connecting the adjacent segments together are molded with 1-junctions. A detailed modeling procedure of the human body musculoskeletal system was presented in [28] and omitted here for the sake of brevity. The complete bond graph model of the proposed musculoskeletal system is depicted in Figure 3.

The governing equations of the musculoskeletal system in the compact form are derived according to the bond graph model represented in Figure 3 and geometrical parameters defined in Figure 2d given by:

$$\begin{cases} \vec{a}_i = -\vec{\alpha}_i \times \vec{R}_{i-} - \vec{\omega}_i \times \left(\vec{\omega}_i \times \vec{R}_{i-}\right) + \vec{a}_{i-1} \\ \vec{F}_i = m_i\vec{a}_i + m_i g\vec{j} + \vec{F}_{i-1} \\ J_i\vec{\alpha}_i = \vec{M}_i - \vec{M}_{i-1} + \vec{R}_{i+} \times \vec{F}_i - \vec{R}_{i-} \times \vec{F}_{i-1} \end{cases} \quad (1)$$

where a_i, α_i, ω_i, F_i, and M_i represent the acceleration, angular acceleration, angular velocity, force and moment of segment i, respectively. The dynamical equations related to the right and left shank, thigh and pelvis could be obtained iteratively employing Equation 1. The dynamic equations corresponding to the right and left feet in the contact phase are given by:

$$\begin{cases} \vec{a}_i = -\vec{\alpha}_i \times \vec{\mathrm{Cop}}_i - \vec{\omega}_i \times \left(\vec{\omega}_i \times \vec{\mathrm{Cop}}_i\right) \\ \vec{F}_i = m_i\vec{a}_i + m_i g\vec{j} + \vec{\mathrm{GRF}}_i \\ J_i\vec{\alpha}_i = \vec{M}_i + \vec{R}_{i+} \times \vec{F}_i - \vec{\mathrm{Cop}}_i \times \vec{\mathrm{GRF}}_i \end{cases} \quad (2)$$

where GRF and Cop represent the ground reaction force and center of pressure under each foot, respectively. Accordingly, the dynamic equations for HAT are expressed by:

$$\begin{cases} \vec{a}_i = -\vec{\alpha}_i \times \vec{R}_{i-} - \vec{\omega}_i \times \left(\vec{\omega}_i \times \vec{R}_{i-}\right) + \vec{a}_{i-1} \\ 0 = m_i\vec{a}_i + m_i g\vec{j} + \vec{F}_{i-1} \\ J_i\vec{\alpha}_i = -\vec{M}_{i-1} - \vec{R}_{i-} \times \vec{F}_{i-1} \end{cases} \quad (3)$$

Since the joint angles between skeletal limb segment, q, serve as the input for graphical representation of movement in a virtual environment, the governing equations

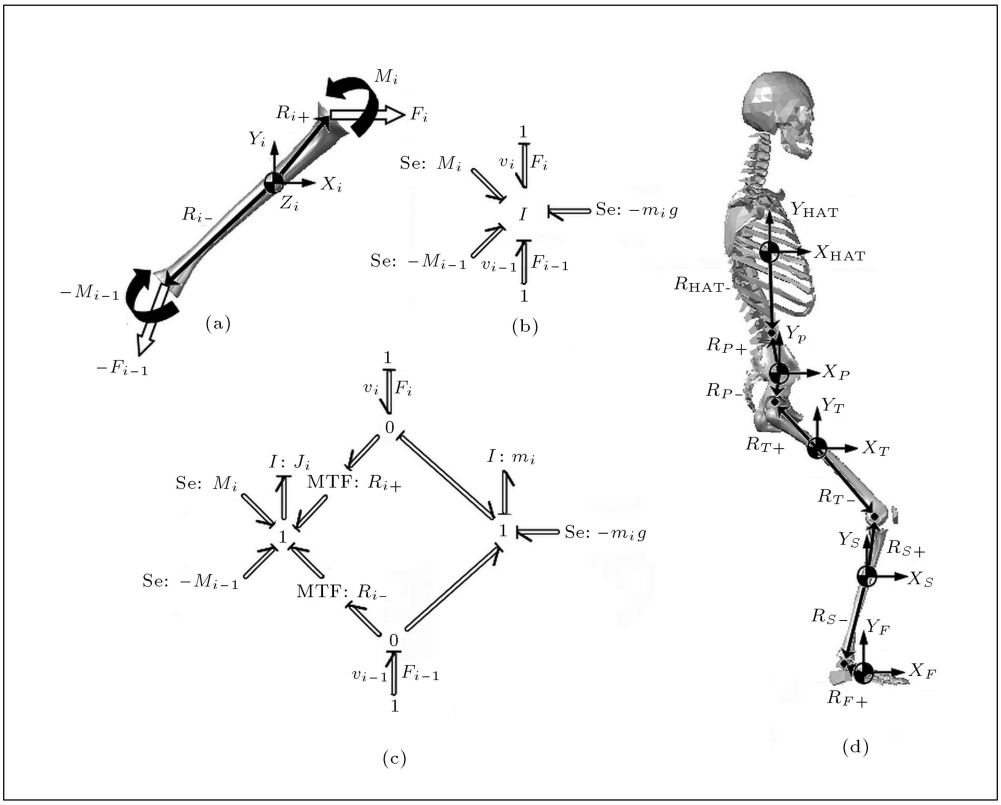

Figure 2. (a) The equivalent force-couple system of ith rigid body; (b) An I field bond graph model representation for ith rigid body; (c) A detailed bond graph model representation for ith rigid body; (d) Definition of the geometrical parameters for a skeletal system.

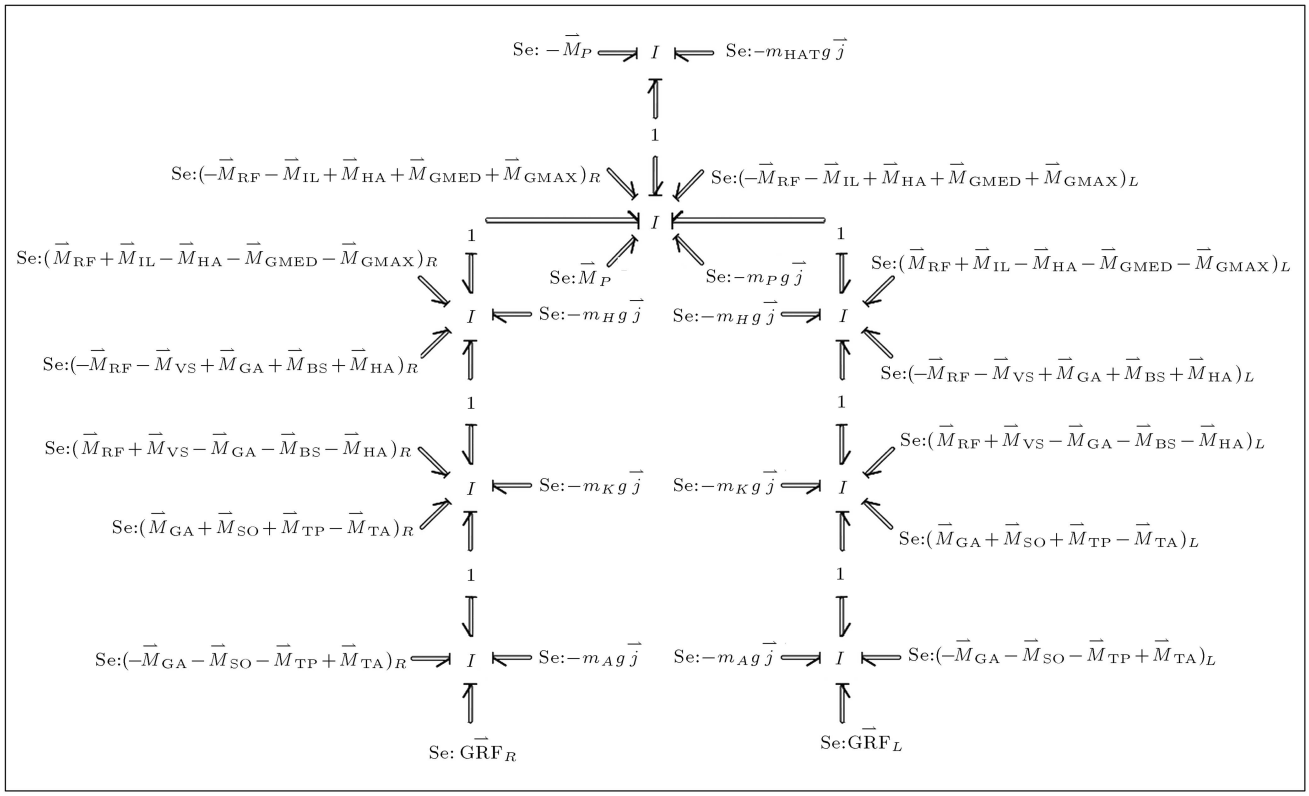

Figure 3. The complete bond graph model representation of the musculoskeletal system.

of motion should be transferred and represented in standard form as:

$$A(q)\ddot{q} + b(q,\dot{q}) + g(q) = R_m(q).F_m + R_{\mathrm{GRF}}.F_{\mathrm{GRF}}, \tag{4}$$

where $A(q)$, $b(q.\dot{q})$, $g(q)$, $R_m(q)$, F_m, R_{GRF} and F_{GRF} are system mass matrix, vector of centrifugal and Coriolis terms, vector of gravity terms, matrix of moment arms about the anatomical joints, vector of muscle forces, matrix of resultant ground reaction force transformation and generalized ground reaction forces, respectively. The muscle activation dynamics were described with a first order differential equation with activation and deactivation time constants of 22 and 200 msec., respectively [24,28]. A computer model of the lower extremity musculoskeletal system was generated employing a block oriented structure of Simulink and integrated with the Virtual Reality toolbox of MATLAB software for graphical representation. The block diagram representation of the complete system is illustrated in Figure 4.

OPTIMIZATION FRAMEWORK

Simulation of the time dependent behavior of human movement was carried out employing the solution of a static or dynamic optimization problem for the redundant muscle groups involved. In this approach, the muscular load sharing problem was solved by minimizing an objective function subjected to a constraint equalizing the sum of individual muscular moments around a joint and the desired joint torques obtained from inverse dynamics. Some additional constraints, such as the final time constraint and muscle force bounds, should be considered in the optimization algorithm. The individual muscle moments around a joint were calculated from the muscle force generated by the optimization routine and the corresponding muscle moment arm which was derived from a musculoskeletal model employing experimental gait data. Performance of the employed method for the estimation of lower extremity muscle forces has been illustrated in the literature extensively [30,31]. Specifically, the performance criterion was considered as the weighted sum of squared residuals in the general form of:

$$J = \sum_{j=1}^{m}\sum_{i=1}^{n} w_j (X_{ij}^{\mathrm{Sim}} - X_{ij}^{\mathrm{Exp}})^2, \tag{5}$$

where X_{ij}^{Exp}, X_{ij}^{Sim}, w_j, m and n are experimentally measured data, simulation data, weighting factor, number of tracking quantities and number of time steps, respectively. Specific quantities evaluated in the objective function include muscle force, muscle stress, joint kinetics, joint kinematics or a combination of

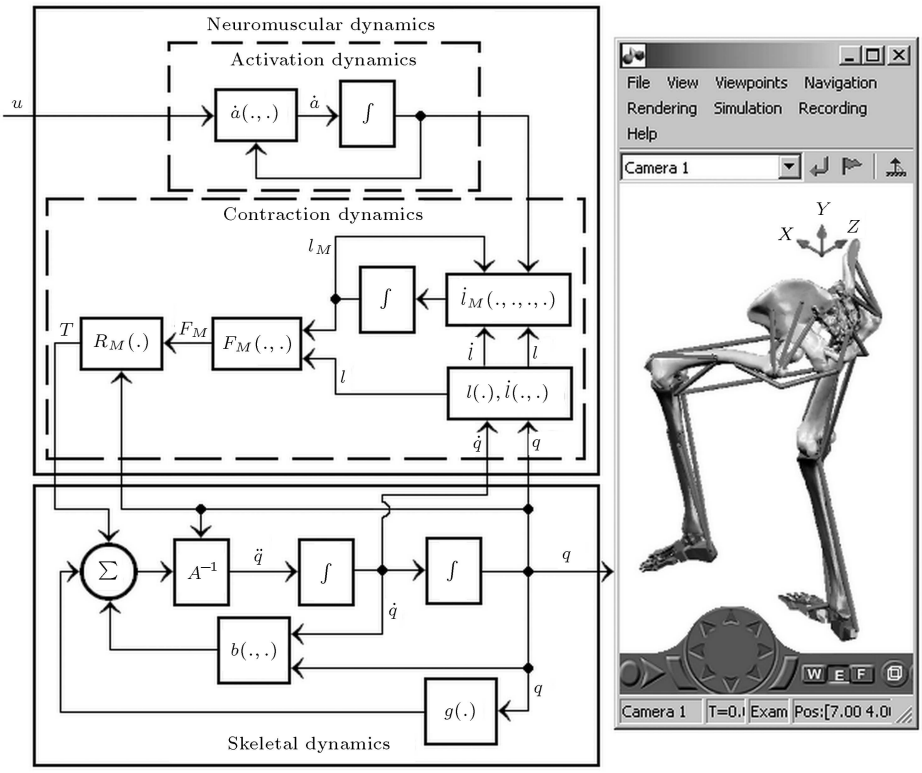

Figure 4. Neuro-musculoskeletal functional block diagram and three-dimensional interactive skeletal model developed in the virtual environment.

them which should be selected appropriately for the movement under investigation.

SIMULATION RESULTS AND DISCUSSIONS

In this study, the inverse dynamics assisted data tracking approach was employed to estimate lower extremity muscle activation during gait in both cases of normal gait and under load carrying conditions. The model anthropometry was set to the average data of five male subjects with an average age, height and weight of 26 ± 3 years, 177 ± 3 cm and 70.1 ± 7.8 kg, respectively, which was reported in [32]. Parameters defining the nominal properties of each actuator, containing peak isometric force, corresponding fiber length and pennation angle of muscle plus tendon slack length, were adapted based on data reported in [23]. Kinetic and kinematical data of the lower extremity related to walking with a 47 kg backpack load and under level walking conditions were extracted from the literature [33] and depicted in Figure 5. Kinematical data was fed into the developed virtual

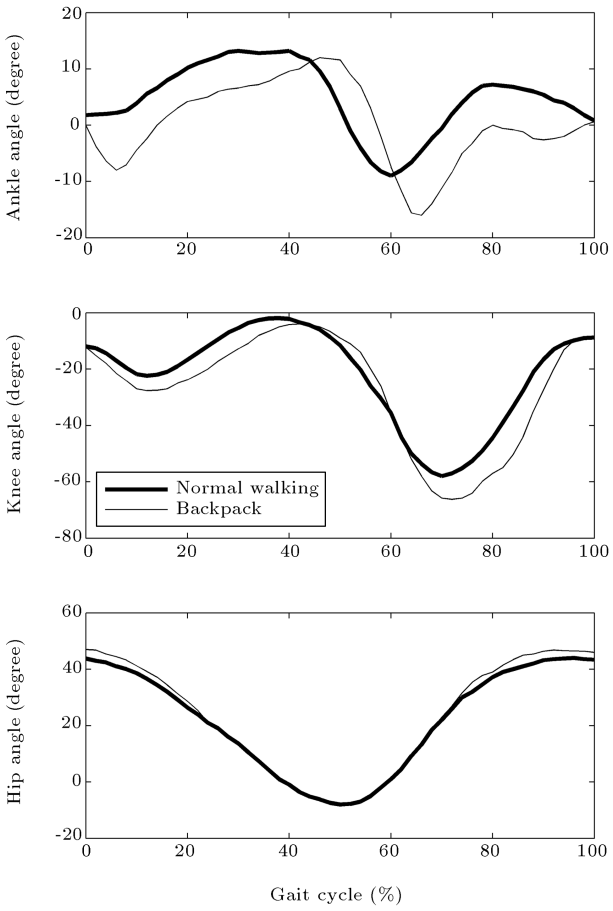

Figure 5. Angular displacement of the ankle, knee and hip joints during normal gait and backpack load carrying based on the data reported in [33].

model of the lower extremity and the moment arm of the lower extremity muscles about the joint for both cases were derived. The computer model of the system [28] was generated, employing a block oriented structure of Simulink, and integrated with the virtual model to perform a dynamic simulation. The inverse dynamics optimization problem for both cases was solved employing a constrained minimization approach. The performance criterion for both cases was formulated to minimize the weighted sum of the muscle activation squared when constrained to track the gait kinetic quantities (i.e. the hip, knee, and ankle joint torques), satisfying the final time constant and muscle activation bound [12]. The excitation pattern for the lower extremity muscles were discretized to 26 points by 50 ms, which were allowed to vary continuously between zero and one. The muscle excitation pattern served as a control parameter in the optimization problem. The algorithm fine-tuned each muscle's excitation onset, duration and magnitude until the sum of the muscle activation squared and subjected to the constraint of joint kinetics over the gait cycle was minimized. An inverse dynamics assisted tracking approach was able to track the experimental joint torques accurately under normal walking and 47 kg backpack load carrying conditions with only a small deviation from the experimental kinetics. Simulated lower extremity joint torques and desired experimental values were illustrated in Figure 6. Estimated muscle excitation patterns for eight of the muscles included in the model under normal walking and 47 kg backpack load carrying conditions were illustrated in Figure 7. The muscle activation patterns are compared with mean (± 1 S.D.) rectified electromyogram (EMG) activities of young adults during normal walking, as reported in the literature [34]. The excitation history of the muscles illustrated that the ankle plantar flexor (SO) and the knee extensor (RF) are the muscles that exhibit a distinct excitation level between normal walking and load carrying. This fact shows the important role of these muscles in the stance phase ($\sim 0 - 60\%$ of the gait cycle). Also, simulation results illustrate that under the load carrying conditions, the primary contributions to body support are provided by hip extensors (GMAX and HA) and the knee extensor (RF) during the loading response phase ($\sim 0 - 10\%$ of the gait cycle). Furthermore, the forward acceleration and deceleration of the body were generated by the knee flexor (BS) during the initial swing phase ($\sim 60 - 70\%$ of the gait cycle) and terminal swing phase ($\sim 85 - 100\%$ of the gait cycle), respectively.

Distribution of muscle mechanical powers under both normal walking and load carrying conditions is illustrated in Figure 8. Power distribution analysis of the muscles reveals that the plantar flexors of the

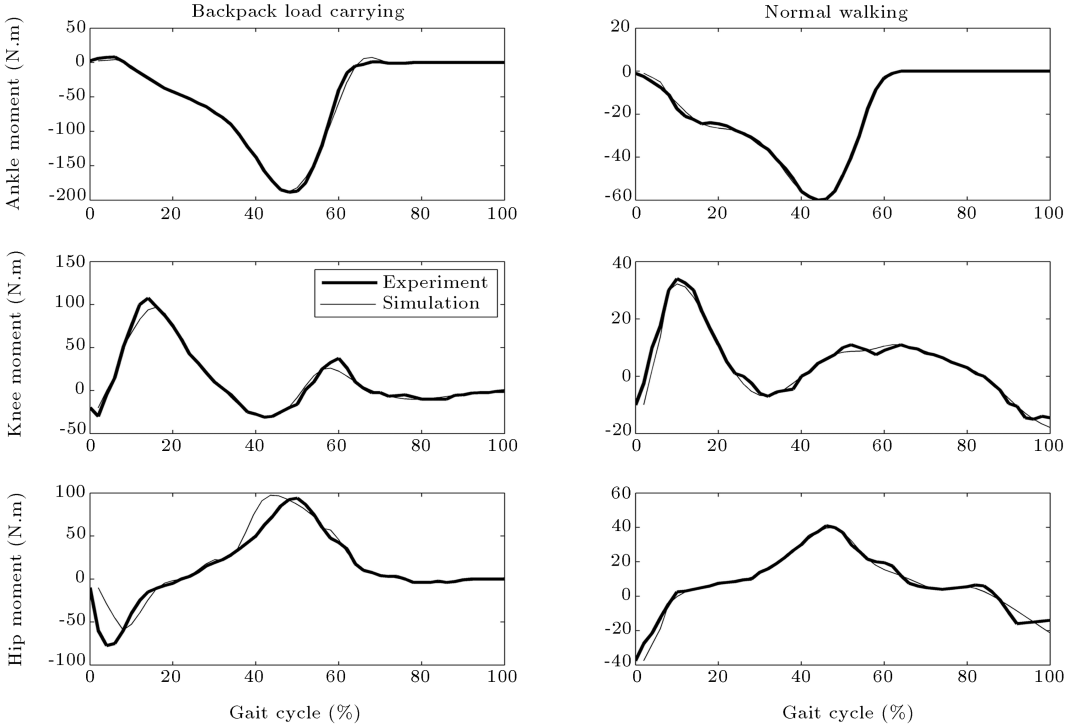

Figure 6. Simulated lower extremity joint torques closely tracked experimental values for normal walking and with 47 kg backpack load carrying condition.

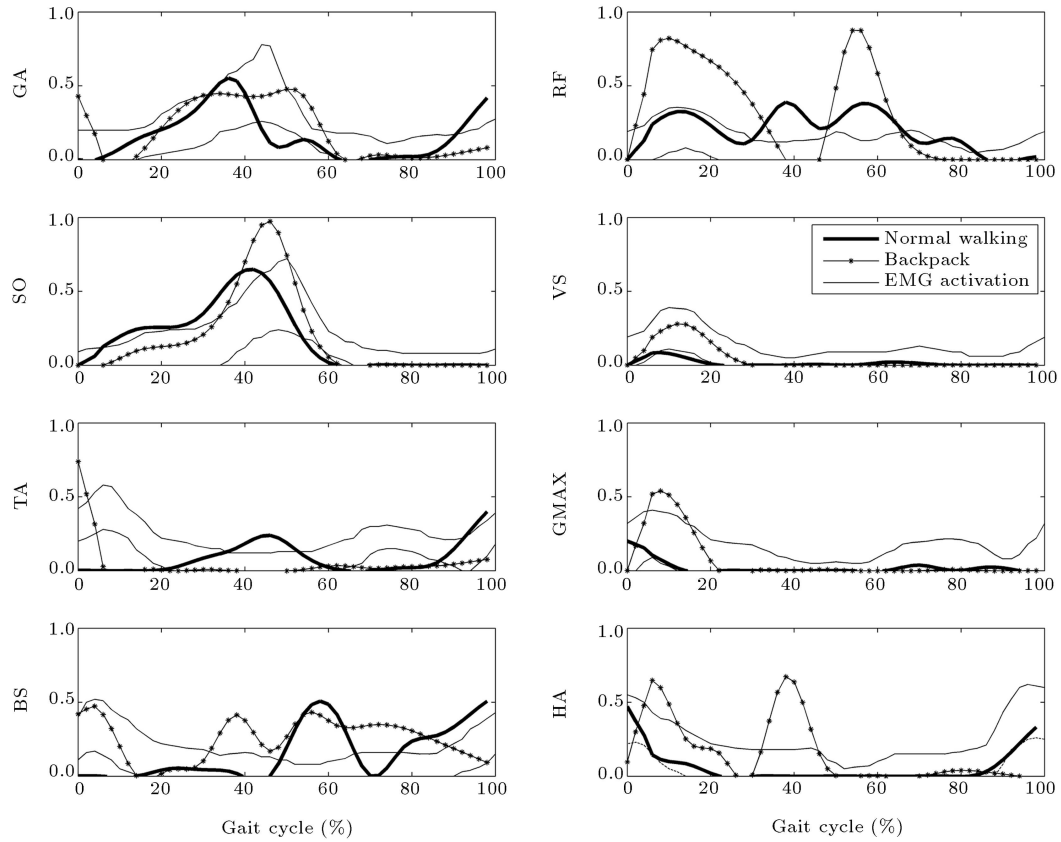

Figure 7. Estimated muscle activation patterns of normal walking and 47 kg backpack load carrying in comparison with the corresponding EMG activities for normal walking reported in [34] for eight of the muscles included in the model.

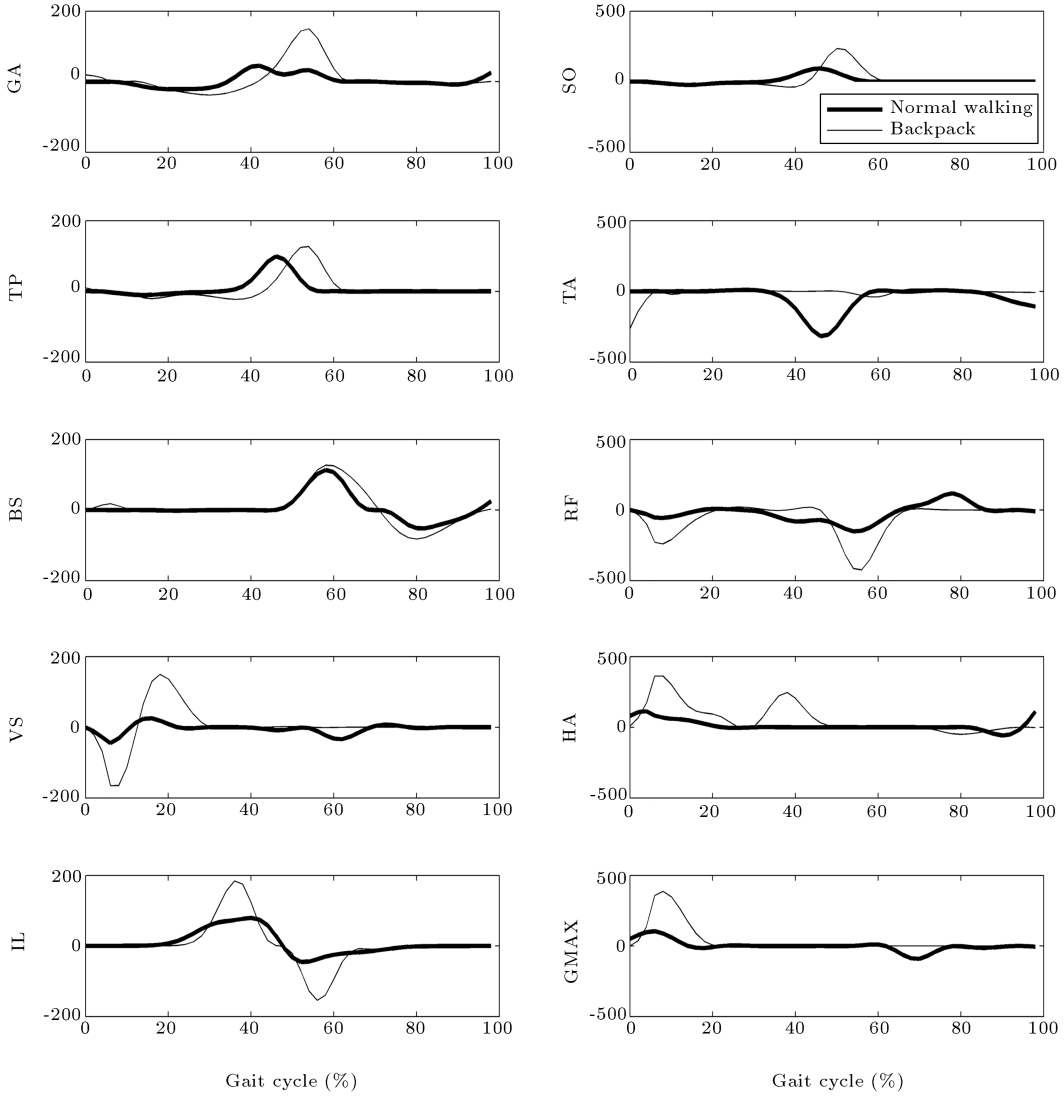

Figure 8. Distribution of the muscle power during normal walking and with 47 kg backpack load carrying conditions. All units are in Watts.

ankle, extensors of the knee and hip joints exhibit distinct functional differences between normal walking and under load carrying conditions. In other words, under the load carrying condition, plantar flexors of the ankle joint transfer the power to support the body during Contralateral Heel-Strike (CHS) to Toe-Off (TO), ($\sim 50-65\%$ of gait the cycle). Furthermore, extensors of the knee joint absorb power during Heel-Strike (HS) to Contralateral Toe-Off (CTO), ($\sim 0-15\%$ of the gait cycle) and transfer the power to support the body during CTO to CHS ($\sim 15-50\%$ of the gait cycle). Additionally, the extensors of the hip joint transfer the power to support the body during HS to CHS ($\sim 0-50\%$ of the gait cycle) and the flexors absorb the power and damp the impact energy during the CHS to TO phase. Besides, the joint power analysis which is depicted in Figure 9, points to the fact that the backpack load did increase joint power as compared to the no load condition. This is reasonable since the added load increases the downward force significantly and translates into larger moments. The role of the ankle joint in transferring power and the knee joint in absorbing power was dominated during CHS to TO. In other words, the ankle and knee joints provide additional effort in supporting the load during CHS to TO. Additionally, the hip joint plays an important role in balancing the transferring and absorbing powers in order to support the load, accelerating and decelerating the body during HS to CHS. In summary, the ankle and knee joints are major contributors in sharing load distribution under load carrying conditions. The moment arms of the muscles about the anatomical joints are another biomechanical aspect that is depicted in Figure 10. The major

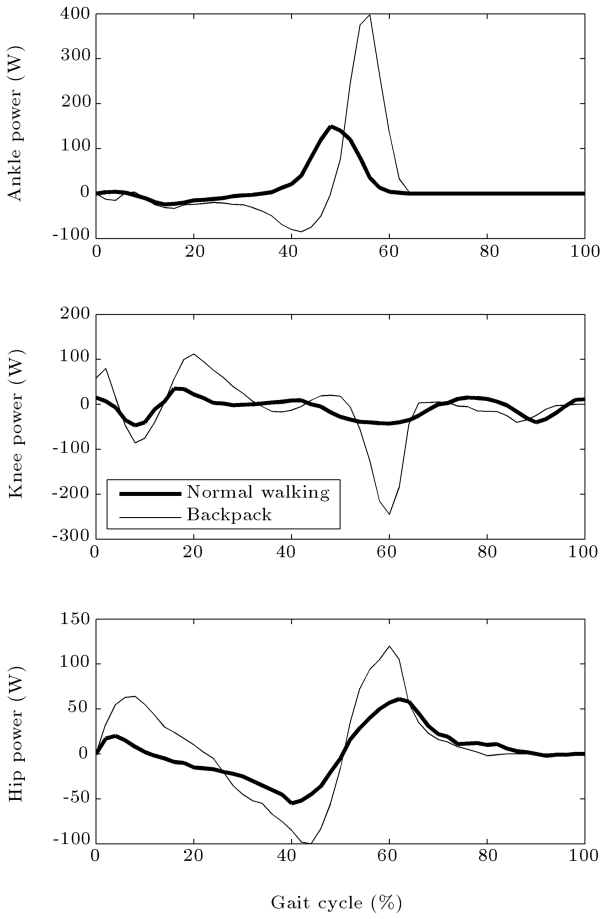

Figure 9. Distribution of the joint powers during normal walking and with 47 kg backpack load carrying conditions.

differences are shown in the moment arm of the muscles about the ankle joint, in a comparison between both cases. This aspect introduces the higher moment production capability of the ankle joint during load carrying.

The overall objective of this study was to gain a deeper understanding of the condition and functioning of the lower extremity muscles during load carrying. Determining in vivo loading conditions in human joints is difficult, due to the combination of complex structural anatomy, complicated movement dynamics and often indeterminate muscle functions. On the other hand, ethical considerations discourage the use of invasive methods to determine muscle forces in humans. Therefore, the only opportunity to estimate the complex distribution of muscle activity is offered by computer simulations. The proposed model offers a powerful computational tool with the aim of employing a block oriented structure of Simulink integrated with the Virtual Reality toolbox of MATLAB software to provide a biomechanical framework for simulating various biomechanical aspects of movement in a virtual environment. In addition, employing a virtual framework analysis makes it possible to evaluate new designed products before construction and is able to perform an optimal design to improve the quality of products. The results of this study will help selecting the proper actuation mechanism of the assistive devices for load carrying purposes. To conclude, the appropriate actuation mechanisms of the assistive devices may include the actuators to provide additional flexion torque for the ankle joint, and an extension torque for the knee and hip joints for the purpose of power augmentation.

CONCLUSIONS

To date, a non-invasive measurement of in vivo muscle forces is still impossible. Ethical considerations discourage the use of invasive methods to determine muscle forces in humans. Therefore, computer simulations offer the only opportunity to analyze the human biomechanical complex. A complete musculoskeletal model of the body, with sixteen musculotendon actuators per leg, was generated with the aim of employing Simulink and the Virtual Reality Toolbox of MATLAB software for this purpose. An inverse dynamics optimization data tracking approach was utilized to estimate the lower extremity muscle load sharing conditions during backpack load carrying. Furthermore, a muscle power consumption analysis was carried out to identify the critical importance and contribution of individual muscles in supporting load during movement. Simulation results illustrate the accuracy and performance of the proposed method to solve muscular load sharing problems during level walking and load carrying. On the other hand, the critical contribution of the plantar flexors of the ankle joint and extensors of the knee and hip joints during load carrying were revealed by the simulation analysis. Biomechanical analysis of the movement under investigation enhances our understanding of human leg morphology and control mechanisms in supporting loads. In addition, by employing a simulation study, it was possible to identify the muscles and joints that are critically subjected to musculoskeletal injury during the activity under investigation. In this case, during load carrying, the dominant roles of the ankle joint in transferring power and the knee joint for its capability of power absorption were highlighted. Besides, muscle energy provides a biomimetic design criterion for anthropometric structures of load augmentation assistive devices. In this case, an additional flexion torque in the ankle joint and an extension torque in the knee and hip joints should be provided by an assistive mechanism. The proposed model can also be employed as a useful tool to provide an appropriate rehabilitation process which can be developed by therapists to improve the gait performance of individuals after musculoskeletal injury.

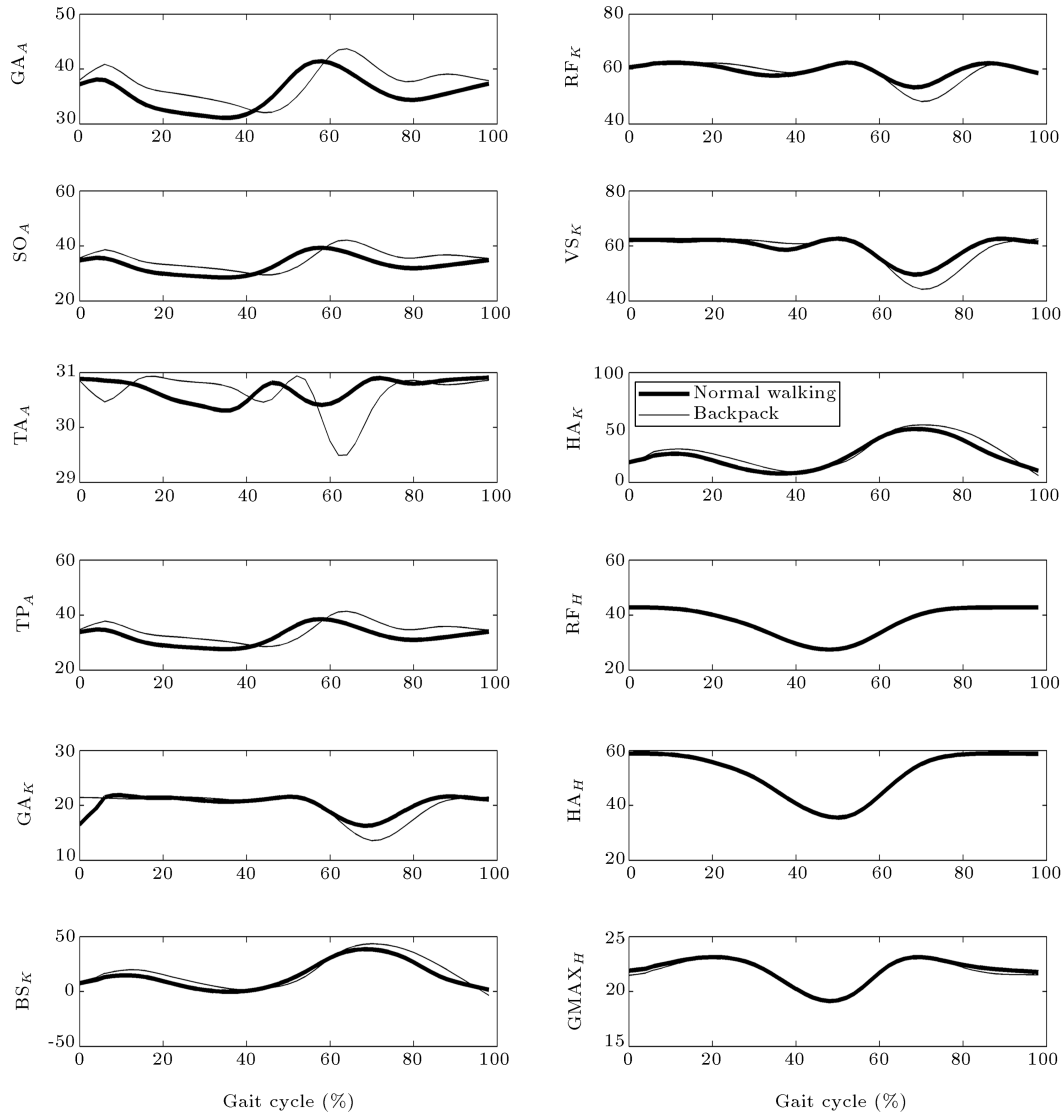

Figure 10. The comparison of the moment arm of the muscles about anatomical joints between normal walking and 47 kg backpack load carrying; subscripts A, K and H stand for the ankle, knee and hip joints, respectively. All units are in mm.

REFERENCES

1. Heller, M.O., Bergmann, G., Deuretzbacher, G., Durselen, L., Pohl, M., Claes, L., Hass, N.P. and Duda, G.N. "Musculoskeletal loading conditions at the hip during walking and stair climbing", *Journal of Biomechanics*, **34**(7), pp. 883-893 (2001).
2. Csintalan, R.P., Schulz, M.M, Woo, J., Mcmahon, P.J. and Lee, T.Q. "Gender differences in patellofemoral joint biomechanics", *Clinical Orthopedics*, **402**, pp. 206-209 (Sep. 2002).
3. Bergmann, G., Graichen, F. and Rohlmann, A. "Hip joint loading during walking and running, measured in two patients", *Journal of Biomechanics*, **26**(8), pp. 969-990 (1993).
4. Nagura, T., Dyrby, C.O., Alexander, E.J. and Andriacchi, T.P. "Mechanical loads at the knee joint during deep flexion", *Journal of Orthopedic Research*, **20**(4), pp. 881-886 (2002).
5. Baltzopoulos, V. "Muscular and tibiofemoral joint forces during isokinetic concentric knee extension", *Clinical Biomechanics*, **10**(4), pp. 208-214 (1995).
6. Crowninshield, R.D. and Brand, R.A. "A physiologically based criterion of muscle force prediction in locomotion", *Journal of Biomechanics*, **14**(11), pp. 793-801 (1981).
7. Zheng, N., Fleisig, G.S., Escamilla, R.F. and Barrentine, S.W. "An analytical model of the knee for estimation of internal forces during exercise", *Journal of Biomechanics*, **31**(10), pp. 963-967 (1998).
8. Anderson, F.C. and Pandy, M.G. "Individual muscle contributions to support in normal walking", *Gait & Posture*, **17**(2), pp. 159-169 (2003).

9. Neptune, R.R., Zajac, F.E. and Kautz, S.A. "Muscle force redistributes segmental power for body progression during walking", *Gait & Posture*, **19**(2), pp. 194-205 (2004).

10. Zajac, F.E., Neptune, R.R. and Kautz, S.A. "Biomechanics and muscle coordination of human walking: Part II: lessons from dynamical simulations and clinical implications", *Gait & Posture*, **17**(1), pp. 1-17 (2003).

11. Anderson, F.C. and Pandy, M.G. "Dynamic optimization of human walking", *Journal of Biomechanical Engineering*, **123**, pp. 381-388 (Oct. 2001).

12. Thelen, D.G. and Anderson, F.C. "Using computed muscle control to generate forward dynamic simulation of human walking from experimental data", *Journal of Biomechanics*, **39**(6), pp. 1107-1115 (2006).

13. Anderson, F.C. and Pandy, M.G. "Static and dynamic optimization solutions for gait are particularly equivalent", *Journal of Biomechanics*, **34**(2), pp. 153-161 (1999).

14. Sasaki, K. and Neptune, R.R. "Differences in muscle function during walking and running at the same speed", *Journal of Biomechanics*, **39**(11), pp. 2005-2013 (2006).

15. Higginson, J.S., Zajac, F.E., Neptune, R.R., Kautz, S.A. and Delp, S.L. "Muscle contributions to support during gait in an individual with post-stroke hemiparesis", *Journal of Biomechanics*, **39**(10), pp. 1769-1777 (2006).

16. Tilbury-Davis, D.C. and Hooper, R.H. "The kinetic and kinematic effects of increasing load carriage upon the lower limb", *Movement Science*, **18**(5), pp. 693-700 (1999).

17. Ren, L., Jones, R.K. and Howard, D. "Dynamic analysis of load carriage biomechanics during level walking", *Journal of Biomechanics*, **38**(4), pp. 853-863 (2005).

18. Abe, D., Yanagawa, K. and Niihata, S. "Effects of load carriage, load position, and walking speed on energy cost of walking", *Applied Ergonomics*, **35**(4), pp. 329-335 (2004).

19. Liu, B.S. "Backpack load positioning and walking surface slope effects on physiological responses in infantry soldiers", *International Journal of Industrial Ergonomics*, **37**(9-10), pp. 754-760 (2007).

20. Hsiang, S.M. and Chang, C. "The effect of gait speed and load carrying on the reliability of ground reaction forces", *Safety Science*, **40**(7-8), pp. 639-657 (2002).

21. Harman, E., Han, K.H., Frykman, P., Johnson, M., Russell, F. and Rosenstein, M. "The effects on gait timing, kinetics and muscle activity of various loads carried on the back", *Medicine and Science in Sports and Exercises*, **24**(5), S129 (1992).

22. Yamaguchi, G.T. and Zajac, F.E. "A planar model for the knee joint to characterize the knee extensor mechanism", *Journal of Biomechanics*, **22**(1), pp. 1-10 (1989).

23. Brand, R.A., Crowninshield, R.D., Wittstock, C.E., Pederson, D.R. and Clark, C.R., van Krieken, F.M. "A model of lower extremity muscular anatomy", *Journal of Biomechanical Engineering*, **104**, pp. 304-310 (1982).

24. Zajac, F.E. "Muscle and tendon: properties, models, scaling, and application to biomechanics and motor control", *CRC Critical Reviews in Biomedical Engineering*, **17**(4), pp. 359-411 (1989).

25. "Virtual Words", in *Virtual Reality Toolbox User's Guide*, Version 4, pp. 5.2-5.21, The MathWorks, Inc., USA (June 2004). Available: www.mathworks.com.

26. Alkjaer, T., Simonsen, E.B. and Dyhre-Poulsen, P. "Comparison of inverse dynamics calculated by two- and three-dimensional models during walking", *Gait & Posture*, **13**(2), pp. 73-77 (2001).

27. Janice, J. and Winter, D.A. "Kinetic analysis of the lower limbs during walking: what information can be gained from a three-dimensional model?", *Journal of Biomechanics*, **28**(6), pp. 753-758 (1995).

28. Selk Ghafari, A., Meghdari, A. and Vossoughi, G.R. "Modeling of human lower extremity musculoskeletal structure using bond graph approach", *CD-ROM Proceedings of ASME International Mechanical Engineering and Exposition*, Seattle, Washington, USA (2007).

29. Margolis, D.L. and Rosenberg, R.C. "Multi-port fields and junction structures", in *System Dynamics: A Unified Approach*, 2nd Edition, p. 244, Wiley, USA (1990).

30. Neptune, R.R. and Hull, M.L. "A theoretical analysis of preferred pedaling rate selection in endurance cycling", *Journal of Biomechanics*, **32**(4), pp. 409-415 (1999).

31. Neptune, R.R., Wright, I.C. and van den Bogert, A.J. "A method for numerical simulation of single limb impact events: Application to heel-toe running", *Computer Methods in Biomechanics and Biomedical Engineering*, **3**(4), pp. 321-334 (2000).

32. Anderson, F.C. and Pandy, M.G. "A dynamic optimization solution for vertical jumping in three dimension", *Computer Methods in Biomechanics and Biomedical Engineering*, **2**(3), pp. 201-231 (1999).

33. Harman, E., Han, K., Frykman, P. and Pandorf, C. "The effects of backpack weight on the biomechanics of load carriage", *USARIEM Technical Report*, Natick, Massachusetts, pp. 100-117 (2000).

34. Winter, A., International Society of Biomechanics, Biomechanical Data Resources, Gait Data. Available: http://www.isbweb.org/data.

APPENDIX A

Included here are the origin and insertion coordinates of the lower extremity muscles included in the proposed musculoskeletal model in Tables A1 and A2.

Table A1. Origin coordinates of the lower extremity muscles included in the proposed musculoskeletal model.

		Coordinates		
Musculotendon Actuator	**Reference Frame**	x **(m)**	y **(m)**	z **(m)**
SO	Talus	-0.0292	0.2467	0.0006
TA	Talus	-0.0155 0.0259	0.2175 0.0257	0.0134 -0.0093
TP	Talus	-0.0268	0.2419	0.0356
GA	Tibia	-0.0203	0.0071	-0.0073
BF	Tibia	-0.0007	0.1784	0.0144
VS	Tibia	0.0106	0.2026	0.0205
RF	Femur	0.0326	0.0323	0.0174
IL	Femur	0.0075	0.1350	-0.0400
HA	Femur	-0.0409	-0.0455	-0.0140
GMAX	Pelvis	-0.1556 -0.1529	-0.0314 -0.1052	0.0058 0.0403

Table A2. Insertion coordinates of the lower extremity muscles included in the proposed musculoskeletal model.

		Coordinates		
Musculotendon Actuator	**Reference Frame**	x **(m)**	y **(m)**	z **(m)**
SO	Foot	-0.0365	-0.0288	0.0056
TA	Foot	0.1850	-0.0510	-0.0330
TP	Foot	0.0715	-0.0420	-0.0260
GA	Foot	-0.0368	-0.0289	0.0028
BF	Talus	-0.0384	0.3323	0.0433
VS	Talus	-0.0005	0.4056	0.0005
RF	Talus	0.0041	0.4084	-0.0006
IL	Tibia	-0.0180	0.3351	0.0116
HA	Talus	-0.0508	0.3321	0.0073
GMAX	Femur	-0.0299 -0.0060	-0.1041 -0.1419	0.0135 0.0411